Transactions of The Indian Institute of Metals
Vol. 62, Issues 4-5, August-October 2009, pp. 337-341

Flow effects on the dendritic microstructure of AlSi-base alloys

Lorenz Ratke, Amber Genau and Sonja Steinbach

Institute for Materials Physics, German Aerospace Centre, DLR, 51147, Cologne, Germany

E-mail: Lorenz.ratke@dlr.de

Received 03 September 2009
Revised 19 October 2009
Accepted 19 October 2009
Online at www.springerlink.com

Keywords:
dendritic solidification; mushy zone; fluid flow; rotating magnetic fields; fractals

Abstract

Fluid flow changes heat and mass transport during solidification, thereby affecting the evolution of the microstructure. In order to quantify effects of convection, it is important that fluid flow can be modified experimentally. We performed directional solidification experiments with binary AlSi alloys of different compositions, using a microgravity environment for diffusive solidification and adding rotating magnetic fields to generate flow. Flow velocities up to 10 mm/s and various solidification velocities were realized while maintaining a constant temperature gradient at the solid-liquid interface. The microstructure observed in samples processed on earth and in space is characterized by primary and secondary dendrite arm spacing and the fractal dimension of the dendrites. It is found that fluid flow usually accelerates growth and coarsening of the dendritic structures and leads to new kinetic laws. The branching of dendritic networks, however, is hardly affected by flow.

Introduction

During the solidification of alloys, constitutional supercooling and morphological instabilities usually lead to the formation of a dendritic network by the solid-liquid interface. This results in a "mushy zone" where the fraction of solid varies continuously in the region between the the liquidus and the solidus or eutectic temperature. The liquid metal between this forest of dendrites (mush) transports solute to the network. Fluid flow is able to drastically modify the species transport in the mush, whose permeability to flow varies with fraction solid and thus temperature from nearly infinite at the tip to zero at its root. Mass transport, however, determines how the dendrite morphology develops. Although a huge amount of research has been devoted to describing the mush or, more generally, porous body permeability, and to flow and mass transport therein [1-11], there are still many open questions [1,9].

We therefore study experimentally the solidification of binary and ternary Al-based alloys subjected to directional solidification in the laboratory and under microgravity. We add fluid flow to the processing parameters in the form of rotating magnetic fields to control the flow experimentally. The response of the microstructure to varying processing parameters is analyzed and referenced to literature models, especially of flow-induced structure changes. The microstructure is analyzed by describing primary stem spacing and secondary dendrite arm spacing, but also by a rarely used method: we analyze the fractal dimension of dendrites. The term *fractal* was coined by French mathematician Benoît Mandelbrot in 1975 [12] to describe self-similar curves or objects whose roughness can not be described by traditional Euclidian geometry. Such shapes can instead be characterized by a non-integer fractal dimension that measures their ability to fill space. A jagged line, for example, will have a fractal dimension between 1 and 2, while a two-dimensional area will have a fractal dimension between 2 and 3.

Materials and methods

Binary AlSi alloys were produced from pure aluminum (99.999%, kindly provided by Hydro Aluminium Deutschland GmbH) and silicon of spectral purity (Crystal Growth Laboratory, Berlin, Germany) and alloyed to give Al with 5, 6 and 9 wt.% Si. Cylindrical samples (diameter 8mm, length 120mm) were solidified directionally upwards in the ARTEMIS facility [13,14] with and without a rotating magnetic field at a constant temperature gradient G of 3K/mm under vacuum conditions. The solidification velocity v was varied in the range of 0.015-0.15mm/s. There are three essential points regarding the ARTEMIS facility. First, there is optical control of the processing due to the use of a transparent crucible material (aerogels). Second, the extremely low thermal conductivity of the aerogels maintains flat isotherms in the samples. Third, due to the aerogel properties a magnetic field device could be brought very close to the sample. The magnetic field device consists of three coil-pairs around the sample powered by a 3-phase current creating a homogeneous rotating magnetic field (RMF). The RMF is able to generate a controlled fluid flow in the whole melt close to the growing solid-liquid interface. The magnetic induction was set to 6mT with the frequency of 50Hz, yielding a magnetic Taylor number of 2200 and a Reynolds number of 0.2 [14]. Special variants of the laboratory ARTEMIS facilities were developed to be used on sounding rockets allowing for the processing of a few samples under microgravity conditions. Details of their technical descriptions can be found in the literature [15-18].

The primary dendrite spacing λ_1 and the secondary dendrite arm spacing λ_2 was measured on metallographic sections perpendicular and parallel to the growth direction [6,19]. In the case of the samples solidified with rotating magnetic field, the spacings were measured in the outer "dendritic ring" of the samples, excluding the eutectic core region at the center which occurred due to macro-segregation

[6,20] at the scale of the sample. Figures of such microstructures with and without a rotating magnetic field and detailes of the measurement method are reproduced and discussed in [6,13,20,31,36] and are therefore omitted here.

In addition we measured the fractal dimension of individual dendrites to analyze if their branched appearance can be characterized by such an analysis and if changes due to fluid flow can be measured. While there are a variety of ways of measuring and defining fractal dimension, we utilize the Minkowski or box-counting dimension, due to its ease of implementation. This value is closely related to the more rigorous Hausdorff dimension [12,21,22].

The fractal dimension was measured on cross sections taken perpendicular to the direction of growth. On each cross section, individual dendrites were identified as shown in Fig. 1. Each dendrite was removed from the image and segmented into a binary image. A one-pixel thick outline of the dendrite was produced using the edge-finding algorithm in Photoshop.

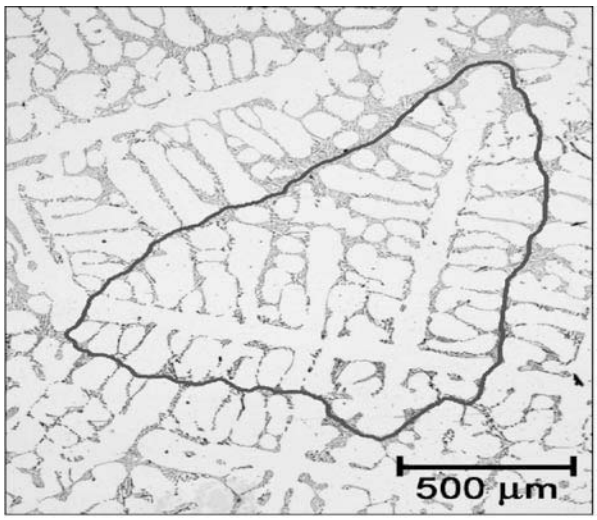

Fig. 1 : Dendritic network on a cross section of an Al-5wt%Si alloy. The white area characterizes the dendritic primary phase. An envelope around the connected primary phase is drawn and used for further analysis.

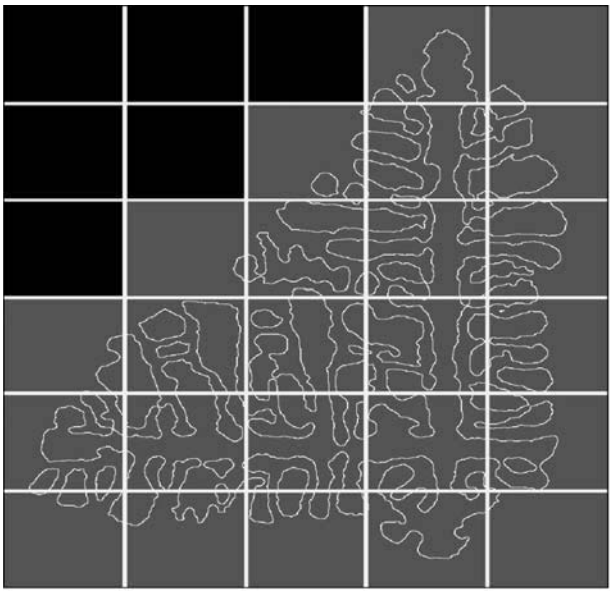

Fig. 2 : A one pixel thick envelope of the dendrite shown in Fig. 1 after orientation parallel to the grid axis. This box covering with different box sizes is used to determine the fractal dimension.

The fractal dimension was calculated as follows. Using a code written in IDL (Interactive Data Language), a grid was placed over the image and the number of boxes required to completely cover the perimeter of the dendrite was determined as shown for one box size in Fig. 2. By varying the grid spacing, a plot is produced, graphing the log of the number of boxes required to cover the dendrite versus the log of the edge length of one box. The Minkowski dimension is defined as one plus the absolute slope of this line [12,21].

Since natural objects can only display fractal qualities over a limited range, the slope was measured from 1.5 to 2.5 (box size of approx. 55 – 550 µm). Fractal dimension is generally assumed to be a valid measure if it remains constant over at least one order of magnitude. Dendrites for which a line could not be fitted in this range with a value of $R^2 \geq 0.990$ were not used.

Results and discussion

The primary dendrite stem spacing changes with solidification velocity with the inverse forth root as expected from classical modeling [2,11,23] as shown in Fig. 3. With increasing silicon content the spacing becomes larger, which simply reflects the reduced amount of primary phase as the alloy moves towards the eutectic composition.

Application of a rotating field of 6mT, which yields flow velocities parallel to the interface of about 10 mm/s and secondary flows in the axial and radial directions of about one mm/s [13] changes the magnitude but not the general relation between spacing, Si concentration and solidification velocity. The models [23-26] all predict a relation of the type

$$\lambda_1 = A\sqrt{c_0}G^{-1/2}\mathrm{v}^{-1/4} = a(c_0)\mathrm{v}^{-1/4} \qquad (1)$$

with A as a constant. Such a function fits very well to the results as shown in Fig. 3. The fit when fluid flow is present is just as good. One can modify this equation by multiplying the forth root of the velocity on both sides yielding a relation

$$\lambda_1 \mathrm{v}^{1/4} = \mathrm{a}(\mathrm{c}_0.\mathrm{RMF}) \qquad (2)$$

in which *a* is a constant depending on Si content and flow velocity. Averaging the expression on the left side for a

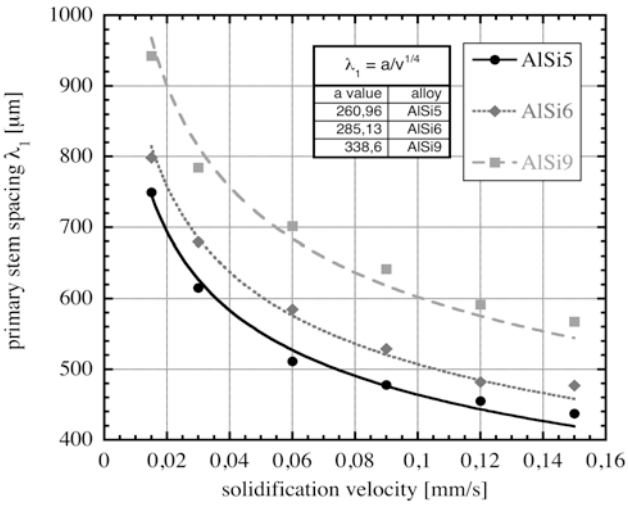

Fig. 3 : Primary dendrite stem spacing in Al-5, 6, and 9 wt.%Si alloys directionally solidified. Curves are fit to the data according to a simple power law predicted by several theoretical models [21-23].

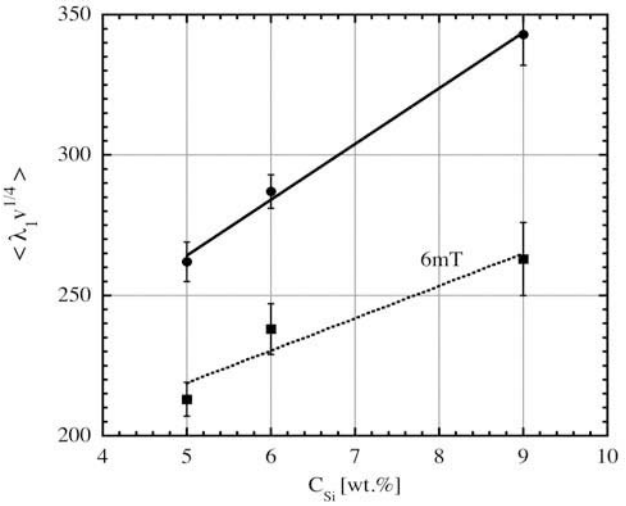

Fig. 4 : Average of the primary spacing multiplied with the forth root of the solidification velocity. The constant of Eq. (2) varies in an almost linear fashion with Si content. According to Eq.(1) a square root dependence would be expected. To discern between a linear and a square root behavior more data points would be needed.

given Si content c_0 and plotting this as a function of Si concentration yields Fig. 4. The data show that with increasing Si content the constant increases in an almost linear manner. The application of rotating magnetic fields reduces the constant but not the functional behavior, reflecting that fluid flow only reduces the primary spacing. This effect is commonly thought to be a result of constitutional supercooling being larger between primary stems [27]. Fluid flow parallel to the dendrite stems enhances the supercooling there, encouraging tertiary arms to grow into primary ones and thus adapting the spacing to the flow-induced supercooling conditions.

All results showing the effect of fluid flow on secondary dendrite arm spacing (SDAS) are presented in Fig. 5. The SDAS increases in both cases with the solidification time, as expected from the models of dendrite arm coarsening [2,3,11,23]. Switching on an RMF field and thus inducing fluid flow yields larger arm spacings and a change in kinetics. Without fluid flow, the SDAS data can be fitted with a cube root of solidification time relation, whereas those data with additional fluid flow are described with a square root relation. Although in the literature the power law $\lambda_2 = M\, t_f^p$ (with p a constant, 1/3 or 1/2) is often modified by adding a constant $\lambda_2 = (\lambda_2^0 + Mt_f)^p$ a careful calculation shows that the conventional models do not allow the addition of such a value [28] and thus the simple power law is correct.

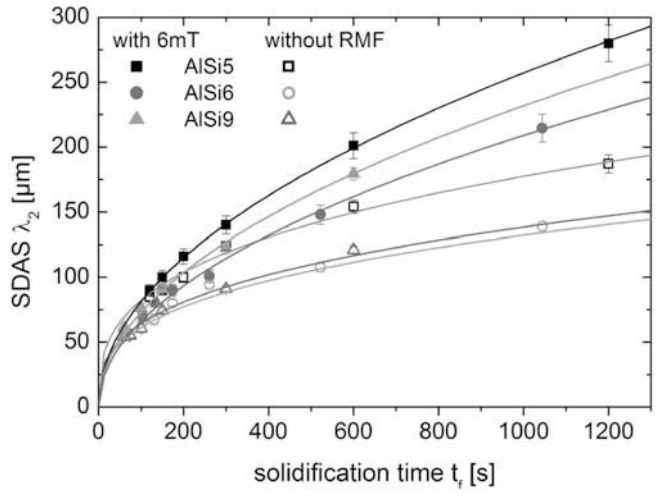

Fig. 5 : Secondary dendrite arm spacing (SDAS) as a function of solidification time for sample processed with and without rotating magnetic fields (RMF) in the laboratory. The data without RMF obey a $\lambda_2 \sim t_f^{1/3}$ relation, whereas those with fluid flow obey a relation $\lambda_2 \sim t_f^{1/2}$.

The effect of flow on the kinetics is shown even more dramatically by comparing the results obtained under microgravity conditions. Fig. 6 shows the results of samples processed under pure diffusive conditions in sounding rocket campaigns TEXUS 39, MAXUS and MAPHEUS and two results from TEXUS 41 and MAXUS with additional fluid flow applied in space (the acronyms are explained in detail in Wikipedia, see [32]). The difference is remarkable and clearly shows that flow not only accelerates coarsening, but also modifies the kinetics.

The change in the kinetics can be understood with a simple model developed by Ratke [29] based on earlier work by Beckermann and co-workers [30] and Ratke and Thieringer [31]. A careful calculation shows that a relation

$$\lambda_2^2 = \frac{1}{2} M \left(\frac{P_R(f_S)\nabla p}{D\eta} \right)^{1/3} t_f = MKt_f \qquad (3)$$

is obtained, in which M is the well-known constant from the diffusive case and contains all aspects of the alloy system used (thermophysical properties and constitution) and K reflects the main assumption that the flow with respect to the dendrite arms can be described as a Stokes flow. P_R is a function describing the permeability as it depends on the fraction solid and ∇_p describes the pressure gradient driving the flow through the mush. D is the diffusion coefficient and η the dynamic viscosity.

As mentioned in the introduction, the description of a dendrite network by just primary and secondary spacing and fraction primary phase does not cover all aspects of dendrite forests. We therefore measured the fractal dimension as a measure of branching and the specific surface area as an integral characteristic of the network.

The Minkowski dimension, d, was calculated for 4-7 dendrites at each solidification velocity, both with and without fluid flow for the Al-5wt.%Si alloy. These values are shown in Fig. 7, with error bars indicating the range within one STD. Within the observed ranges, δ does not change

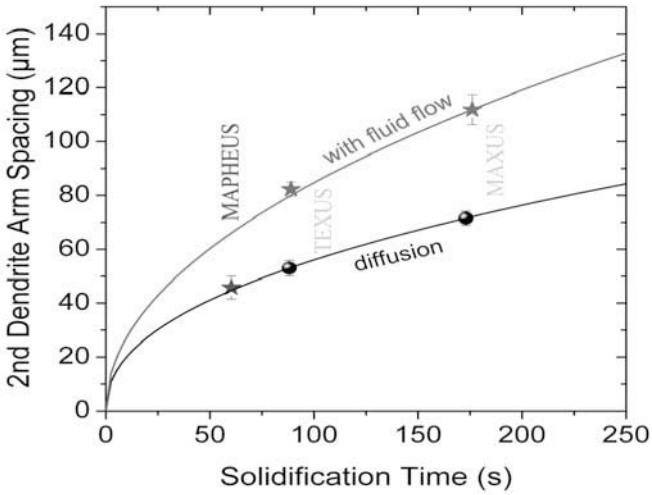

Fig. 6 : SDAS of samples process under microgravity conditions with and without additional fluid flow by RMF.

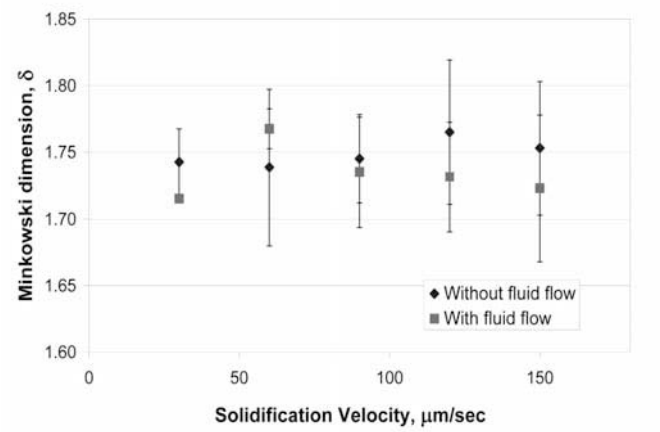

Fig. 7 : Fractal dimension (Minkowski) for dendrites in Al-5wt.%Si as a function of different solidification velocities, with and without fluid flow.

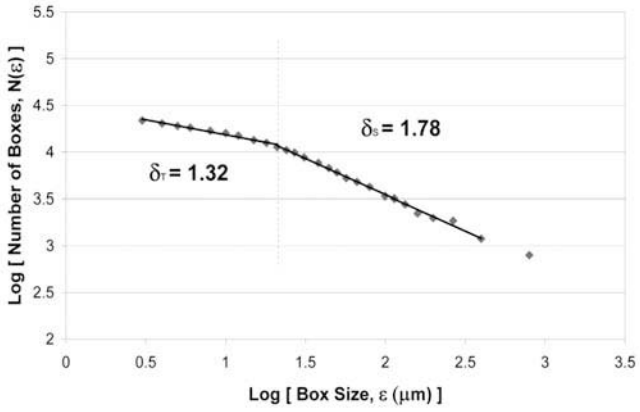

Fig. 8 : Double logarithmic plot showing that in a certain range of box sizes covering the dendrites, two different slopes can be attained, attributed with a structural aspect of dendrites (the δ_S value) and surface roughness characterized by the δ_T value.

with either solidification velocity or the addition of fluid flow. The average value measured for all dendrites is 1.74 ± 0.06.

For some dendrites, two linear regions were apparent. These two regions have been identified by Kaye [21] as the structural fractal (δ_S) and the textural fractal (δ_T), were δ_S gives information about the overall morphology of the object and δ_T about the surface roughness. The textural Minkowski dimension was measured for 13 dendrites and ranged from 1.15 to 1.34.

Despite the inherent difficulties and some inaccuracies in determining the fractal dimension, our results indicate that fluid flow does not affect branching significantly nor does the solidification velocity within the ranges being measured modify the average fractal dimension. Other measurements of fractal dimension of dendrites for comparison are relatively scarce in literature. Bilgram *et. al.* [33] measured the projected outline of Xenon dendrites using both the box counting and the so-called correlation method, and found $\delta = 1.42 \pm 0.05$, independent of solidification velocity and coarsening time, which is in agreement with our findings. Yang *et. al.* [34] report $\delta = 1.228 - 1.418$ for a directionally solidified Ni superalloy, with the fractal dimension increasing with solidification velocity, although reporting fractal values to such an artificially high precision indicates a misunderstanding of the nature of such measurement.

That the fractal dimension, and thus the nature of dendrite branching, does not change with fluid flow and processing parameters is on first sight unexpected, since fluid flow is known to drastically accelerate dendrite arm coarsening (see above) and the transformation of a mush to a compact solid body [35]. Therefore we expected that in samples processed with magnetic fields a lower fractal dimension would be measured. The absence of such a change might give a hint that, for the given parameters, fluid flow only changes the scale of the dendrites, but not the branching and compactness. Thus the fractal dimension might not be a sensitive measure to mush changes. Analysis of the fractal dimension for the other alloys reported here is currently in progress.

References

1. Beckermann C, *Int. Mat. Rev.,* **47** (2002) 243.
2. Kurz W and Fisher D J, *Fundamentals of Solidification*, Trans Tech Publ., Ackermannsdorf, (1989).
3. Flemings M C and Nereop G E, *Trans. AIME,* **239** (1967) 1449.
4. Davidson P A and Boysan F, *Appl. Sci. Res.,* **44** (1987) 241.
5. Hainke M, Friedrich J and Müller G, *J. Mat. Sci.,* **39** (2004) 2011.
6. Steinbach S and Ratke L, *Mat. Sci.* Eng. A, **413-414** (2005) 200.
7. Heinrich J C and Poirier D R, *Comptes Rendus Mecanique,* **332** (2004) 429.
8. Poirier D R, *Metall. Mater. Trans. B,* **18** (1987) 245.
9. Erdmann R G, Poirier D R and Hendrick A G, *Mat. Sci. Forum,* in press
10. Churchill S W, *Viscous Flow*, Butterworths, Boston (1988)
11. Dantzig J and Rappaz M, *Solidification*, EPFL Press, Lausanne, Switzerland (2009)
12. Mandelbrot B B, *Fractals: Form, Chance and Dimension,* Freeman, San Francisco (1977)
13. Steinbach S and Ratke L, *Mat. Sci. Forum,* **508** (2006) 491.
14. Hainke M, *Computation of convection and alloy solidification with the software package CrysVUn*, Univ. Erlangen-Nuremberg, Germany, (2004).
15. Ahrweiler S, Ratke L and Masslow H D, Proc. 16th Symp European Rocket and Balloon Programmes and Related Research, 2 - 5 June 2003, St. Gallen, Switzerland, ESA SP-530, 107-112, ESA Publications Division ESTEC, Noordwijk, Netherlands
16. Steinbach S, Ratke L and Masslow H D, Proc. of the 17th Symp. on European Rocket and Balloon Programmes and Related Research, Sandefjord, Norway, ESA SP-590, (2005) 521.
17. Steinbach S and Ratke L, Proc. 18th ESA Symposium on European Rocket and Balloon Programmes and Related Research, Visby, Sweden, 3-7 June 2007, ESA SP-647, Noordwijk, Netherlands, (2007) 373.
18. Stamminger A, Ettl J, Blochberger G, Drescher J, Griesche A, Hoepfner S, Hörschgen M, Meyer A, Neumann C, Ratke L, Plescher E and Willnecker R, Proc. ESA Symposium on European Rockets and Balloon Programmes, Bad Reichenhall 2009, ESA SP, in press
19. Mason J T, Verhoeven J D and Trivedi R, *J. Cryst. Growth.,* **59** (1982) 516.
20. Steinbach S, Ratke L, *J. Cast. Met. Res.,* **20** (2007) 140.
21. Kaye B H, *A Random Walk Through Fractal Dimensions*, VCH Publishers, New York (1989).
22. Soltzberg L J, Fappiano S A, Hidek L E, O'Brian M J, Suarez L L, *Acta Cryst.,* **48A** (1992) 457.
23. Sahm P R, Egry I, Volkmann T, *Schmelze, Erstarrung und Grenzflächen*, Vieweg, Braunschweig (1999)

24. Hunt J D, *Solidification and Casting of Metals,* **192** (1979) 3, The Metal Society, Ohio
25. Fisher D J, Kurz W, *Acta Metall.,* **29** (1981) 11.
26. Trivedi R, *Metall. Trans.,* **A15** (1984) 977.
27. Beckermann C, Diepers H-J, Steinbach I, Karma A and Tong X, *J. Comp. Physics*, **154** (1999) 468
28. Ratke L, Berg- und Hüttenmännische Monatshefte BHM, **154** (2009) 107.
29. Ratke L, Steinbach S, Proc. 5th Decennial Conf. Solidification Processing, Sheffield 2007, H. Jones, Ed, University of Sheffield, GB, (2007) 14.
30. Diepers H-J, Beckermann C and Steinbach I, *Acta Mater.,* **47** (1999) 3663.
31. Ratke L and Thieringer W K, *Acta Metall.,* **33** (1985) 1793.
32. http://en.wikipedia.org/wiki/Maxus_(rocket)
33. Bisang U and Bilgram J H, *J Cryst. Growth,* **166** (1996) 207.
34. Yang A, Xiong Y and Liu L, *Sci. Tech. Adv. Mat.,* **2** (2001) 101.
35. Kasperovich G and Ratke L, Steinbach S, *J. Cast. Met. Res.,* **22** (2009) 151.
36. Steinbach S, Kapserovich G and Ratke L, *Trans. Ind. Inst. Metals,* **60** (2007) 103.